

Solid fraction determination via DSC analysis

G. Gottardi, A. Pola, G.M. La Vecchia

The solid fraction trend as a function of temperature, $F_s(T)$, is an important parameter in different sectors of metallurgy: from the study of the rheological behaviour of alloys to the simulation of foundry processes as well as in the semi-solid forming techniques. The thermal analysis, in particular the differential calorimetric one (DSC), can represent an optimal tool for measuring the actual solid fraction of an alloy. As known DSC results depend on the used test parameters (sample mass and heating rate), on the calorimetric tracings and on the peaks interpretation. The aim of the present work is the identification of test conditions that allow to better estimate the solidification phenomenon thus to make the DSC analysis a reliable tool for the $F_s(T)$ definition.

The A356 aluminium alloy was used for the DSC analyses.

The experimental data obtained, varying the heating rate and the sample mass, were compared to those calculated by simulation obtained using CompuTherm Database® and Pandat® software.

Keywords: Semi-solid - Solid fraction - DSC

INTRODUCTION

The use of a metallic alloy in an intermediate state between liquid and solid condition, called semi-solid, represents from several years a turning point in foundry techniques.

The term semi-solid alloy indicates a metallic suspension characterized by a solid primary phase, typically with globular shape, surrounded by a liquid matrix (generally eutectic).

A semi-solid is characterized by a flow behaviour extremely dependent from solid fraction, shear rate and time (non-Newtonian fluid). If compared to conventional casting techniques, where fully liquid metal is poured or injected into the die cavity, in semi-solid processing the higher viscosity of the material reduces the stochastic turbulent phenomena and gas entrapment during die filling, resulting in a higher quality casting. In addition, reduced volumetric shrinkage during solidification with respect to conventional casting methods and lower tendency to gas enrichment (hydrogen and oxygen) allow the obtainment of sound castings [1].

Advantages can be reported also in the case of hot plastic deformation processes. In fact, the semi-solid technology ensures the production of complex shaped parts with reduced loads and number of forming steps, as a consequence of the small percentage of liquid that makes the material more easily deformable.

In both cases the knowledge of the trend of solid fraction with temperature, $F_s(T)$, is extremely important for both semi-solid casting and forming or to perform rheological

measurements, aimed at understanding the behaviour of the alloy in the semi-solid range. This parameter often is not present in the material databases and, therefore, it has to be determined experimentally or via calculation.

H.V. Atkinson et al. (2005) studied the link between chemical composition and solid fraction, for both a foundry (A356) and a wrought alloy (2014) [2]. They showed the importance of having a solid fraction versus temperature curve not too steep, to avoid for small changes in temperature an excessive increase of the solid fraction percentage that can prevent the proper die filling. This trend can be determined, once known the chemical composition of the alloy, using a series of predicting models which assume particular conditions of solidification [3]. Other methods are based on indirect measurements that require an appropriate calibration and interpretation of the experimental data. One of the most widely used methods is the thermal analysis via the DSC (Differential Scanning Calorimetry) [4]. A proof of the reliability of DSC investigation with analytical solution, based on Scheil's equation, and image analysis with proper corrections has been proved by Zavaliangos et al. (2000) [5] on aluminium silicon and aluminium magnesium alloys.

To date there are no existing standards which define the test conditions for the solid fraction determination. The literature shows the use of different scanning rates β , mainly in the range of 5-20 K min⁻¹.

Torres et al. (2013) [6] showed the effect of composition on F_s by comparing the DSC results, at two levels of solid fraction (45-60%), and those obtained via theoretical model. In such research they investigated two heating rate (5 and 20 °C/min) finding that DSC resulting temperatures are higher (from 9 to 16 °C) than the calculated ones. Rogal et al. (2010) [7] determined the liquid fraction

G. Gottardi, A. Pola, G.M. La Vecchia

*DIMI, University of Brescia
gianmaria.gottardi@unibs.it*

trend and the correct process temperature by testing a 100Cr6 steel for thixoforming applications via DSC analyses. In this study the heating process was carried out for scanning rate of 20 K min⁻¹. Similarly Rassili and Atkinson (2010) [8] identified, in relation to Kazakov criteria [9], the range of workability for different steels destined to thixo-forming applications, using DTA measurements at about 10 K min⁻¹. Battezzati et al. (2000) [10] determined the characteristic temperatures and solid fraction for a cast iron, during melting and solidification, with a scanning rate of 10 K min⁻¹. Pola et al. (2008) [11] verified the characteristic temperatures and peaks for an aluminium thixo-casting alloy (AlSi5Mg0,5Cu0,3Ag) at 5 K min⁻¹ of scanning rate. Birol (2009) [12] shows, for an A357 alloy, how the data concerning the characteristic temperatures, eutectic and liquidus, and the solid fraction can be influenced by the heating and cooling rate during the test. In particular considering the heating mode, Birol deduced how scan rate of 0,5 K min⁻¹ may lead to an underestimation of the data of the solid fraction, while higher velocity to an overestimation. Opposite situation can be found using cooling tests.

It has to be noticed that during a DSC test the heat flow curve commonly suffers from a thermal delay (thermal lag) between the set test temperature and the recorded one. This delay is often related to the thermal resistance between the sample and the sensor, due to the heat transfer by conduction. It determines a temperature gradient in the measuring system which causes the distortion of the DSC path shape. This leads to errors in the determination of partial areas corresponding to the percentage of completed transformation, which corresponds to the solid fraction during the liquid-solid transition [4, 13]. Additionally, as well known, the result of a DSC test is extremely dependent on several parameters, as for example on the sample mass and on the heating rate used [14]. In particular, the “zero line” or “Baseline” is conditioned significantly by the scanning rate and by furnace atmosphere and the extent of its flow; the final shape of the peak is influenced by the sample conductivity/heat capacity, its mass and the heating rate. However, up to now, it is still not clear the determination of the liquidus temperature and solid fraction trend for low percentages which are of high interest in some semi-solid applications. The aim of this work is to define a proper test reference procedure able to guarantee a good reproducibility and reliability of the data.

EXPERIMENTAL

The tests have been performed on A356 samples obtained from commercial cast ingot whose chemical composition is shown in Table 1. It consists in a conventional aluminium foundry alloy free of modifiers or refiners. Liquidus and eutectic temperatures as well as the $F_s(T)$ have been measured using a DSC TA Q600 instrument equipped with software Universal Analysis 2000 acquisition system. The tests have been carried out in a pure argon controlled

Si	Fe	Cu	Mg	Zn	Ni	Cr	Al
7.4700	0.1267	0.0023	0.2120	0.0077	0.0016	0.0028	Bal.

Table. 1 - Chemical analysis composition of the tested A356 alloy (wt %).

atmosphere for different values of heating rate, between 0.5 and 25 °C/min (in detail 0.5, 1, 2, 5, 10, 15, 20 and 25 °C/min), using two masses for the samples, i.e. 10 and 20 mg. The A356 samples have been melted within alumina crucibles and the DSC analyses have been conducted with a test procedure defined directly by the calorimeter software. The test procedure consists in a ramp at a fixed heating rate. In particular, an initial conditions balancing at 50 °C, followed by data acquirement up to the temperature of 710 °C (about 50 °C higher than the pure aluminium melting temperature) to guarantee the fully occurrence of the liquid/solid transformation. An average values of liquidus-eutectic temperatures and solid fraction behaviour has been taken as the result of three DSC analysis per testing condition.

RESULTS AND DISCUSSION

Examples of some thermograms obtained by DSC analyses of the A356 alloy melting are reported in Fig. 1. The heat flow curve is formed by two endothermic peaks which represent the eutectic and the liquidus temperature. Formation of secondary phases can lead to a change in the signal, especially at high scanning rate: using an alloy with a low amount of added elements prevents such occurrence.

The correct definition of solidus and liquidus temperatures is extremely important to set the integration interval necessary to identify the solid fraction trend with temperature.

As shown in Fig. 1, for analogue heating rates and changing the mass, the curves undergo a small change in the baseline value and a more marked variation in the entity of the heat flow (peak) changing the scanning rate. Contrary to this with a constant mass, a high heating rate increases the measurement sensitivity reducing the temperature accuracy and resolution [15]. This problem is mainly due to the thermal delay (inertia) in the transmission of heat between the furnace and the sample, especially at high temperatures.

The transition between the solid and the liquid phase, as widely described in the literature, begins at the temperature of onset of the first endothermic peak and ends at the peak temperature of the last endothermic transformation reported in the heat flow curve [12, 13]. According to that the identified characteristic temperatures are reported in Tab. 2.

It can be observed that the relative value in the alloy melting range remains almost the same, independently from the heating rate and sample mass used in the analysis: average values of 35.28 °C (standard deviation 1.95 °C) for tests carried out on the 10 mg samples and 33.45 °C (standard

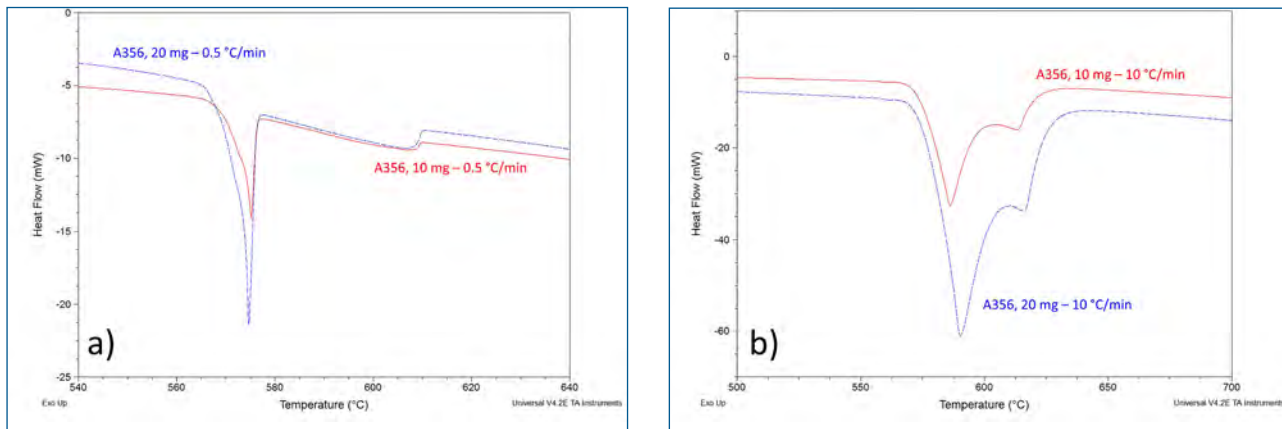


Fig. 1 - Thermograms concerning the tests performed on the A356 alloy at 0.5 °C/min (a) and 10 °C/min (b).

β [°C/min]	Sample 10 mg		Sample 20 mg	
	T onset eutectic [°C]	T peak liquidus [°C]	T onset eutectic [°C]	T peak liquidus [°C]
0.5	573.24	607.18	573.41	606.55
1	573.42	609.03	574.80	609.03
2	573.70	610.97	575.11	610.76
5	576.09	609.83	578.05	612.34
10	576.30	612.97	580.37	615.70
15	581.62	616.41	588.74	620.67
20	579.03	617.02	588.71	620.86
25	586.70	618.96	588.91	619.79

Tab. 2 - Liquidus and eutectic temperatures measured for the 10 and 20 mg samples at different scanning rates.

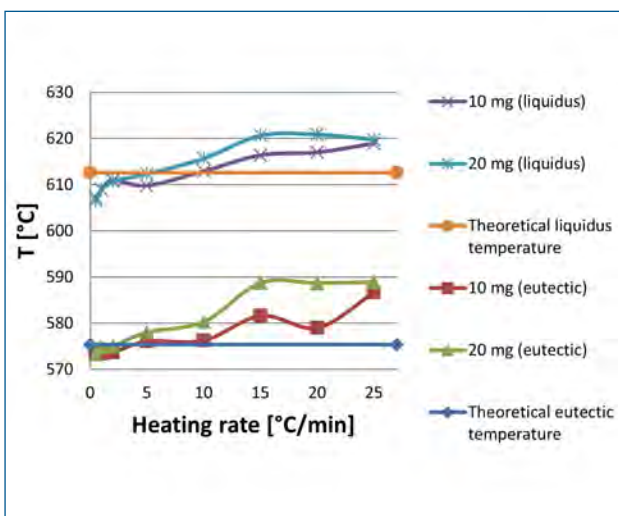


Fig. 2 - Eutectic and liquidus temperatures Vs heating rate.

deviation 1.71 °C) for the analysis performed with 20 mg. The experimental data trend shows that an increase in β leads to higher detected temperatures but to a lower thermal inertia related to the sample mass.

The experimental results were compared with the calculated data, using the simulation software Pandat 8.1[®], for the lever rule and Gulliver-Scheil model as well as CompuTherm Database, available in Procast[®], by using the Back-diffusion model with a cooling rate of 0.5 K/s.

These models gave values of eutectic phase and liquidus formation almost similar and respectively equal to 575.4 °C and 612.6 °C. Fig. 2 shows the trend of the liquidus and eutectic temperatures, measured varying the heating rate, compared to the corresponding calculated values.

It can be clearly seen that the characteristic transformation temperatures tend to increase with the heating rate and mass used: behaviour predictable and completely consistent with the previously made assumption of thermal inertia between the calorimeter and the sample [13, 14].

Regarding the eutectic formation, a scanning rate lower than 10 °C/min ensures a good approximation of the forecast temperature, especially at low sample mass: the 10

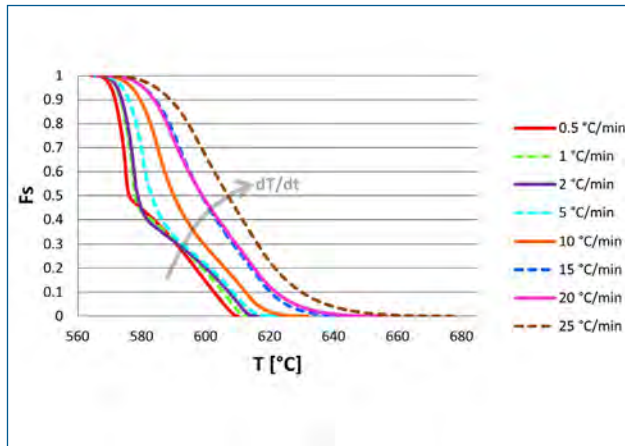


Fig. 3 - Solid fraction Vs Temperature graphs for 10 mg samples.

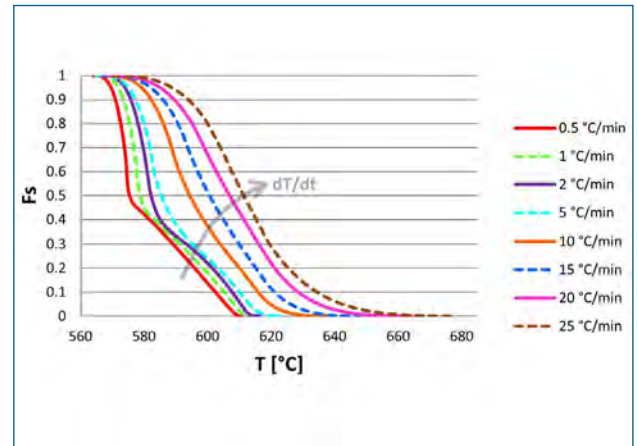


Fig. 4 - Solid fraction Vs Temperature graphs for 20 mg samples.

mg mass provided more stable data the higher the heating rate. Similarly in the case of liquidus: the temperature tends to be better approximated for scan rate of 5 and 10 °C/min, respectively for the masses of 10 and 20 mg. In both cases lower rates lead to a slight underestimation of the expected data, opposite case for higher rates.

The correct identification of the eutectic and liquidus is extremely important for the determination of the starting and ending integration points of the thermogram.

Through the integration of the heat flow curve it's possible to identify the percentage of transformed phase: being a melting process, we obtain the liquid fraction (ones' complement of the solid fraction). The liquid fraction, in fact, corresponds to the area subtended under the baseline described by the thermogram chart. In Figs. 3-4 the results of the solid fraction trend with temperature measured via DSC are shown for each test condition.

For both the tested masses, the $F_s(T)$ undergoes a shift along the temperature axis with the increasing of scanning rate due to the existing system thermal delay (sample-crucible-thermocouple). Additionally, it can be seen that the results, for β in the interval of 0.5-5 °C/min, are independent from mass. The graph of Fig. 5 shows the trend of the curves of temperature Vs solid fraction forecast from the three examined models.

The Lever rule, in the hypothesis of equilibrium solidification, and Gulliver-Scheil model, under the assumption of alloy elements diffusion only in the liquid, although providing the same value of eutectic and liquidus temperature, differ in the solid fraction description with temperature [3]. Similar considerations can be applied to the Back-Diffusion model: it derives from the evolution of the Gulliver-Scheil model which takes into account a possible, albeit limited, diffusion in the solid phase [16]. The trends of these curves reflect the hypothesis that underpin the above mentioned models: although they provide the same value of eutectic and liquidus temperature, they differ in the solid fraction description with temperature especially near the eutectic phase formation, at around 46% of solid fraction, up to the solidus temperature.

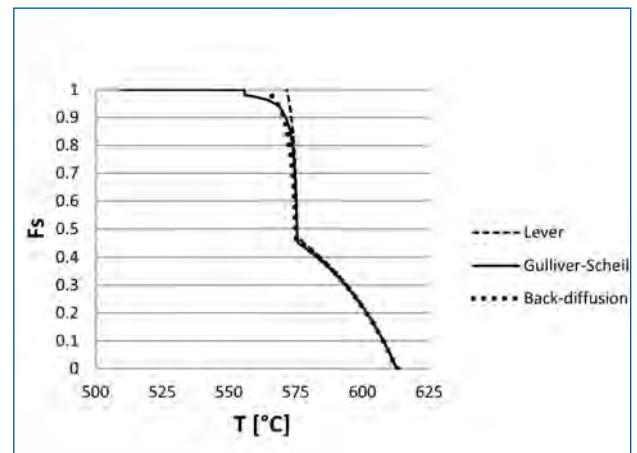


Fig. 5 - Solid fraction Vs temperature forecast from the lever rule, Gulliver-Scheil e Back-diffusion models.

Based on these considerations, the trend of solid fraction with temperature was split into two main areas, pre and post eutectic formation, and analyzed separately for the scanning rates which provided the more stable data, 0.5-1-2-5 °C/min (Fig. 6).

In relation to the charts of Fig. 6 (a) and (b), related to the stage preceding the eutectic formation, it can be observed that, for both masses, the trends described from the experimental data comply with those predicted by the above discussed models.

The expected temperature for a fixed F_s , regarding the 10 mg tests, shows a standard deviation of 2 °C, for tests performed at 0.5-1-2 °C/min, and about 4 °C for tests conducted at 5 °C/min. Similarly for 20 mg tests mass, the standard deviation is about 2 °C for $\beta = 1-2$ °C/min, 3 °C for $\beta = 0.5$ °C/min and about 6 °C for the tests conducted at 5 °C/min. In both cases, a scanning rate of 5 °C/min, despite suffering from a higher temperature data error, shows an excellent approximation of the solid fraction data in the range between 10 and 30%.

For both the analyzed masses, the $F_s(T)$ tends to be better

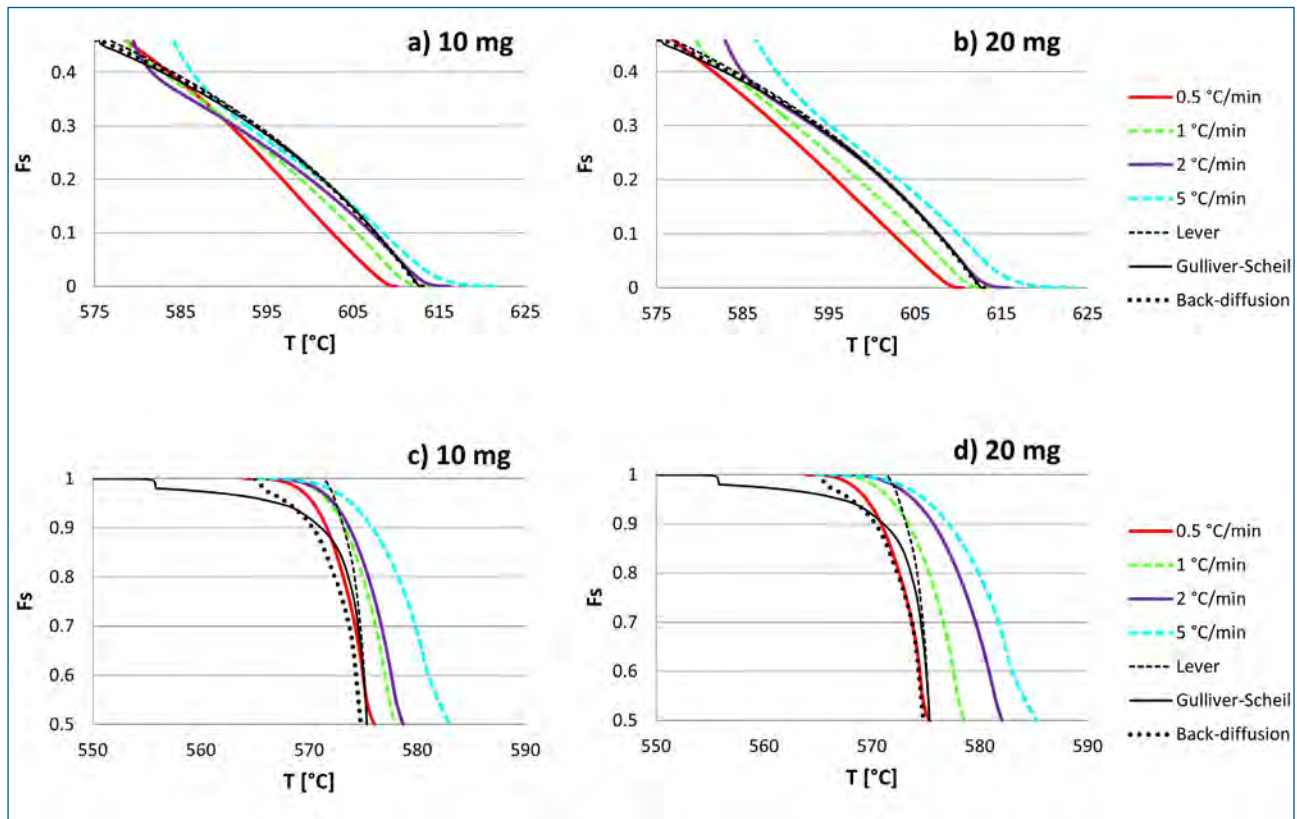


Fig. 6 - F_s Vs T graphs forecasted from Lever, Gulliver-Scheil and Back-diffusion model. a, b - Pre-Eutectic formation (10 - 20 mg); c, d - Post-Eutectic formation (10 - 20 mg).

defined at heating rate of 0.5 °C/min for values of solid fraction percentage between 50% and 70%, which is the upper limit for thixoforming processes [1] (Fig. 6 (c) and (d)). In this interval, for a fixed value of theoretical F_s , the 0.5 °C/min rate ensures a variability of the temperature data that reaches the maximum of 0.6 °C. Higher heating rates lead to a significant deviations in the experimental data compared to those predicted by the lever, Gulliver-Scheil and Back-Diffusion models: this phenomenon is amplified from the heating kinetics and the tested mass, reaching values even higher than 8 °C.

It can be stated that the more suitable DSC test conditions are those that are affected by minor data deviation and system thermal inertia. Tests carried out with lighter masses and low scanning rates return values consistent with those predicted by the considered theoretical models.

CONCLUSIONS

In the present work a series of DSC tests were carried out on a A356 alloy in order to find out a reliable test procedure, comparing the measurements through the use of theoretical models (Lever, Gulliver-Scheil and Back-diffusion). It was found that the measured eutectic and liquidus temperatures tend to follow the calculated data when lower masses (10 mg) and heating rate lower than 10 °C/min are used. Heating rates higher than 5 °C/min lead to the achievement of a solid fraction curve which

overestimates, for a fixed temperature, its extent respect to that expected from theoretical models. $F_s(T)$ charts, for scanning rate between 0.5 and 5 °C/min and up to solid fractions of thixo-forming interest (up to $F_s = 0.7$), better approximate experimental data as the masses and test rate appear to be lower. The optimal test condition was found to be 10 mg with heating rate of 5 °C/min. The value is reduced to 0.5 °C/min, for a better $F_s(T)$ approximation, in the case of values of $F_s > 0.5$.

The obtainment of a precise value, whether it be the solid fraction or eutectic-liquidus temperature, is deemed extremely important in all the applications where is required a certain degree of accuracy: for instance thixo-forming, rheological measurements, welding, etc..

REFERENCES

- 1] G. Hirt, R. Kopp, Thixoforming, John Wiley & Sons, Weinheim, 2009, pp. 1-27.
- 2] D. Liu, H. V. Atkinson, H. Jones, Thermodynamic Prediction of Thixoformability in Alloys Based on the Al-Si-Cu and Al-Si-Cu-Mg Systems, Acta Materialia 53 (2005) 3807-3819.
- 3] D. M. Stefanescu, Science and Engineering of Casting Solidification (Second Edition), Springer, New York, 2009, pp. 33-47.
- 4] R. B. Cassel, Determining Percent Solid in a Polymer Blend, TA Instruments.

- 5] A. Zavaliangos, J.C. Lin, M. Yin, Microstructure and rheology of two new aluminium alloys for semisolid processing, *Semi-solid processing of alloys and composites* (2000) 463-468.
- 6] L.V. Torres, E.J. Zoqui, Characterization of the microstructure and rheological behaviour of Al-4wt%Si-2.5wt%Cu alloy produced by direct chill casting and electromagnetic stirring, *Solid State Phenomena* 192-193 (2013) 142-148.
- 7] L. Rogal, J. Dutkiewicz, T. Czeppe, J. Bonarski, B. Olszowska-Sobieraj, Characteristics of 100Cr6 bearing steel after thixoforming process performed with prototype device, *Transactions of Nonferrous Metals Society of China* 20 (2010) s1033-s1036.
- 8] A. Rassili, H. V. Atkinson, A review on steel thixoforming, *Transactions of Nonferrous Metals Society of China* 20 (2010) s1048-s1054.
- 9] A. A. Kazakov, Alloy compositions for Semisolid Forming, *Advanced Materials & Processes* 157 (2000) 31-34.
- 10] L. Battezzati, M. Baricco, F. Marongiu, G. Serramoglia, D. Bergesio, Melting and solidification studies by advanced thermal analysis of Cast Iron, *Metallurgical Science and Technology* 19 (2001) 16-20.
- 11] A. Pola, R. Roberti, M. Modigell, L. Pape, Rheological Characterization of a New Alloy for Thixoforming, *Solid State Phenomena* 301 (2008) 141-143.
- 12] Y. Birol, Solid fraction analysis with DSC in semi-solid metal processing, *Journal of Alloys and Compounds* 486 (2009) 173-177.
- 13] R. B. Cassel, How Tzero™ Technology Improves DSC Performance Part V: Reducing Thermal Lag, *TA Instruments*.
- 14] G. Höhne, W. Hemminger, H. J. Flammersheim, *Differential Scanning Calorimetry*, Springer Science & Business Media, Berlin, 2003, pp. 31-63.
- 15] R. B. Cassel, High Heating Rate DSC, *TA Instruments*.
- 16] M. Trepczyńska-Łent, Solidification with back-diffusion of irregular eutectics, *Archives of Foundry Engineering* 8 (2008) 117-120.